Cell. Mol. Life Sci. 65 (2008) 3861 – 3871
1420-682X/08/233861-11
DOI 10.1007/s00018-008-8339-0

Cellular and Molecular Life Sciences

Research Article

ERK activation by Ca^{2+} ionophores depends on Ca^{2+} entry in lymphocytes but not in platelets, and does not conduct membrane scrambling

A. Arachiche[a, b,†], I. Badirou[a,†], J. Dachary-Prigent[b], I. Garcin[c], D. Geldwerth-Feniger[a] and D. Kerbiriou-Nabias[a,*]

[a] INSERM U770 and Université Paris-Sud, 80 rue du Général Leclerc, 94276 Le Kremlin-Bicêtre cedex (France), Fax: +33-1-4671-9472, e-mail: daniele.kerbiriou-nabias@inserm.fr
[b] INSERM U688 and Université Victor Segalen, Bordeaux (France)
[c] INSERM UMR-S757 and Université Paris-Sud, Orsay (France)

Received 18 June 2008; received after revision 24 September 2008; accepted 1 October 2008
Online First 16 October 2008

Abstract. Rapid Ca^{2+}-dependent phospholipid (PL) reorganization (scrambling) at the plasma membrane is a mechanism common to hematopoietic cells exposing procoagulant phosphatidylserine (PS). The aim of this research was to determine whether activation of the extracellular signal-regulated kinase (ERK) pathway was required for PL scrambling, based on a single report analyzing both responses induced by Ca^{2+} ionophores in megakaryoblastic HEL cells. Ca^{2+} ionophore-stimulated ERK phosphorylation was induced in platelets without external Ca^{2+}, whereas exogenous Ca^{2+} entry was crucial for ERK activation in Jurkat T cells. In both cells, membrane scrambling only occurred following Ca^{2+} entry and was not blocked by inhibiting ERK phosphorylation. Furthermore, ERK proteins are strongly phosphorylated in transformed B lymphoblastic cell lines, which do not expose PS in their resting state. Overall, the data demonstrated that ERK activation and membrane scrambling are independent mechanisms.

Keywords. Extracellular signal-regulated kinase, phosphatidylserine, phospholipid scrambling, platelet, Jurkat, B lymphocytes, Scott syndrome.

Introduction

Phospholipid (PL) reorganization (scrambling) with translocation of phosphatidylserine (PS) to the external leaflet of cell membranes occurs in apoptosis and during blood coagulation [1, 2]. PS exposure, required to clear apoptotic debris, can be slow (several hours) in apoptotic situations [3]. Conversely, PS is exposed in minutes in response to stimuli such as thrombin or collagen in blood platelets and Ca^{2+} ionophores in platelets and other hematopoietic cells [4, 5]. The negatively charged platelet surface forms docking sites, which catalyze the formation of complexes essential for blood coagulation, leading to thrombin formation (reviewed in [1]). PS translocation is accompanied by the shedding of microparticles, which also expose a negatively charged procoagulant surface [4, 5].

The essential role of PL reorganization on the surface of stimulated blood cells is illustrated by Scott syndrome, a rare bleeding disorder [6, 7]. Platelets,

† These authors contributed equally to this work.
* Corresponding author.

erythrocytes, and Epstein-Barr virus (EBV)-immortalized B lymphocytes (B lymphoblasts) from these patients all exhibit defective membrane scrambling when challenged by Ca^{2+} ionophores, despite a normal Ca^{2+} influx [7–13].

The Ca^{2+}-dependent mechanisms underlying rapid PL redistribution at the membrane include a variety of events, such as activation of transmembrane outward PS transporters (reviewed in [14]), inhibition of the inward aminophospholipid translocase [4, 15], and PS transmembrane redistribution due to the cell shrinkage that modifies lipid packing in both leaflets [16]. In lymphocytic cells, the increase in intracellular Ca^{2+} concentration ($[Ca^{2+}]_i$), e.g., as induced by thapsigargin, is not sufficient to provoke scrambling [11, 13, 17]. These results suggest that Ca^{2+} ionophores induce an additional, unknown signaling that is required for membrane scrambling.

Only a limited proportion of platelets exhibit rapid PS translocation when activated with thrombin or collagen *in vitro* [5, 15, 18]. In contrast, in platelets and lymphocytes, Ca^{2+} ionophores (ionomycin or A23187) efficiently induce membrane PL reorganization of the whole population [5, 9, 13, 17]. Knowledge of the particular signals, defective in Scott cells, underlying Ca^{2+} ionophore-induced membrane scrambling is therefore a motivating goal for the understanding of blood hemostasis regulation.

Experimental data in human erythroleukemia (HEL) cells suggested that extracellular signal-regulated kinase (ERK) phosphorylation by Ca^{2+} ionophore A23187 was involved in the PS translocation mechanism [19]. The mitogen-activated protein kinase (MAPK)/ERK pathway is crucially involved in regulating growth and differentiation in a variety of cells (reviewed in [20]). In this pathway, two proteins, ERK1 (p44) and ERK2 (p42), which share 88 % identical sequences, are phosphorylated by their upstream kinases MEK1 and MEK2. Phosphorylation sites include a threonine (Thr, T) and a tyrosine (Tyr, Y) residue. ERK1/2 proteins act as a point of convergence for multiple intracellular signaling pathways in response to different external stimuli.

Anucleated platelets have no growth potential, and are thus useful cells for studying the involvement of ERK in cell signaling independently of DNA-related pathways. The MAPK/ERK pathway contributes to several platelet responses such as those implicating, in aggregation or thrombosis, the membrane glycoprotein receptors involved in platelet adhesion to subendothelial components [21–24]. Thrombin, collagen and Ca^{2+} ionophores rapidly activate ERK phosphorylation in isolated platelets [25–30]. However, the involvement of the MAPK/ERK pathway in the PL scrambling induced by these agents had not previously been studied in platelets.

This work presents a detailed analysis of ERK activation in relation to PL scrambling, in T and B lymphoblastic cells and platelets activated by Ca^{2+} ionophores. Besides platelets, Jurkat T and B lymphoblasts are also relevant models for exploring the mechanisms underlying PS translocation [9, 10, 13, 17, 31, 32]. We demonstrated that ERK phosphorylation was induced by Ca^{2+} ionophores in a cell-specific manner, requiring external Ca^{2+} influx in Jurkat cells, but occurring in platelets without Ca^{2+} entry. Ionophore-induced PL scrambling was stimulated by an external Ca^{2+} influx in both cell types. Plasma membrane PL reorganization still occurred when the MAPK/ERK pathway was inhibited. Our data suggested that independent intracellular signals promote Ca^{2+} ionophore-stimulated ERK phosphorylation and plasma membrane scrambling.

Materials and methods

Reagents and materials. Fura-2/AM (Fura-2) and FM1–43 were purchased from Molecular Probes; Annexin A5-FluoProbes 488 and the Annexin A5 binding buffer (containing 2.5 mM $CaCl_2$) were from FluoProbes; U0126, PD98059, Bromo-A23187 and ionomycin were from Calbiochem (Merck biosciences); X-VIVO 15 culture medium for lymphocytes, containing 1.8 mM Ca^{2+}, was from BioWhittaker; RPMI 1640 glutamax-1 culture medium, nonessential amino acids, sodium pyruvate, gentamicin and phosphate-buffered saline (PBS) were from Gibco; fetal calf serum (FCS) was from PAA; the kit for quantifying protein concentrations in lymphocyte cell lysates was from Sigma; the lysis buffer provided in a phospho-MAPK array kit, the affinity-purified polyclonal antibodies (Abs) against doubly phosphorylated ERK1 and ERK2 (anti-pT202/Y204 ERK1/pT185/Y187 ERK2) and the monoclonal Ab directed against both ERK1 and ERK2 (anti-ERK1/2) were from R&D Systems; the monoclonal anti-pY-ERK1/2 Ab was from Santa Cruz; the horseradish peroxidase (HRP)-conjugated goat anti-mouse IgG was provided by R&D Systems or Jackson Immuno-Research; HRP-conjugated goat anti-rabbit IgG was from Santa Cruz (sc-2004) or Jackson Immuno-Research; electrophoresis and transfer devices were Mini Protean 3 from Bio-Rad or XCell *SureLock* Mini-Cell and XCell II Blot Module from Invitrogen; transfer membranes for Western blots were from GE Healthcare; HRP was revealed on the Western blots using WesternGlo from R&D Systems, SuperSignal West Pico Chemiluminescent substrate from Pierce, or the

ECl-Plus Kit from GE Healthcare; ready-to-use gels and buffers for electrophoresis and Western blotting were provided by Bio-Rad or Invitrogen; all other reagents for buffers were from Sigma Chemicals, Carlo Erba, or Merck.

Cells and culture conditions. Jurkat E6–1 human leukemia T cells were obtained from ATCC and cultured in complete RPMI medium [RPMI glutamax-1 supplemented with 1% (v/v) nonessential amino acids, sodium pyruvate (1 mM), gentamicin (20 μg/ml), and 10% (v/v) FCS]. EBV-transformed B lymphocytes (B lymphoblasts) from a French patient with Scott syndrome, presumably homozygous for the mutation, were established in our laboratory and characterized, as previously detailed [10]. Scott B lymphoblasts were cultured in X-VIVO 15 culture medium. Control B lymphoblasts from unrelated healthy donors were established in our laboratory and cultured either in X-VIVO 15 or complete RPMI media.

Ca^{2+} ionophore activation conditions. In the literature, micromolar range of either Ca^{2+} ionophore A23187 [1, 5, 10], or ionomycin [11, 13, 15, 17] have been used to stimulate membrane scrambling in platelets, erythrocytes or lymphocytes. Several parameters, including Ca^{2+} and ionophore concentrations, are essential to the process. It has been demonstrated that ionomycin, A23187 and Bromo-A23187, all exhibit the same Ca^{2+} transport properties [33]. Our experimental conditions were based on our previously published studies showing that efficient membrane scrambling occurs for the whole population of platelets upon stimulation with 3 μM bromo-A23187 [5], and for the whole population of lymphoblasts with 2 μM ionomycin [13].

Dual measurement of $[Ca^{2+}]_i$ and plasma membrane remodeling in Jurkat cells by fluorescence imaging video microscopy. Jurkat cells were cultured in suspension at 2×10^5 cells/ml and used 24 or 48 h later. For video microscopy experiments, the cells were centrifuged at 220 *g* for 10 min and suspended at 10^6 cells/ml in X-VIVO 15 culture medium containing the Ca^{2+} probe Fura-2 (4 μM). A 500-μl sample of the cell suspension was layered onto poly-L-lysine-coated round glass slide for 40 min at 37°C. The attached cells were washed three times with the lymphocyte reaction buffer containing 116 mM NaCl, 1.8 mM $CaCl_2$, 5.6 mM KCl, 1.2 mM $MgCl_2$, 5 mM $NaHCO_3$, 1 mM NaH_2PO_4, and 20 mM HEPES, pH 7.3, or without $CaCl_2$ in the presence of 0.1 mM EGTA [13]. The slides were then set between adapted metal circles to form an observation chamber. Reaction buffer (500 μl) containing 5 μM FM1–43 was added to the cells. FM1–43 is a styryl dye that fluoresces under interaction with anionic PL at the external membrane layer [34] and used to monitor membrane remodeling. The chamber, maintained at 37°C, was positioned under the microscope equipped with a video camera. Fura-2 and FM1–43 fluorescence were recorded simultaneously every 4 s and, as previously described, images were analyzed by drawing regions of interest over single cells [13]. Emitted light was collected with a 515-nm dichroic mirror and a 520-nm longpass filter. Excitation at 450–490 nm enabled us to determine the increases in FM1–43 fluorescence. Increases in $[Ca^{2+}]_i$ were shown by the ratios of Fura-2 fluorescence under excitation at 340 nm *versus* 380 nm. For purposes of statistical analysis, individual cells treated similarly in at least three independent experiments performed on different days were taken into account to calculate averages. The results are expressed as means ± standard deviation.

Activation of lymphocyte cells for ERK1/2 phosphorylation and Western blot analysis. Cells were seeded 24 h before the experiments at 2×10^5 Jurkat/ml or 3×10^5 B lymphoblasts/ml. Immediately before the experiments, the cells were centrifuged, suspended at 10^7cells/ml in different volumes of reaction buffer, depending on the experiments, and warmed for 5–10 min at 37°C. A 1-ml aliquot of the cell suspension was then withdrawn at different time points, before (time "0") and after addition of 2 μM ionomycin, and immediately centrifuged for 7 min at 220 *g*. The cells were then suspended in 500 μl lysis buffer, agitated for 30 min at 4°C, and centrifuged (14 000 *g*, 5 min at 4°C) to eliminate the cell debris. When 10 μM U0126 was used, it was added to the cells for 20 min prior to activation with ionomycin. For Western blotting, the lymphocyte cell lysates (20 or 30 μg protein, in similar amounts for all samples on a given gel) were diluted to 40 μl with PBS in 1× Laemmli buffer (62.5 mM Tris-HCl, pH 6.8, 2% SDS, 10% glycerol, and 0.002% bromophenol Blue), heated at 90°C for 5 min, subjected to 10% SDS-PAGE and transferred to the membrane. Buffers and gels were provided by the manufacturers [excepted for the transfer buffer used with the Bio-Rad apparatus: 192 mM glycine and 25 mM Tris, pH 8.3, 20% (v/v) methanol]. Western blotting was performed with the appropriate primary and secondary HRP-conjugated Abs and detected using chemiluminescent substrates.

Analysis of externalized PS by Annexin A5 staining using flow cytometry. At the same time as the Jurkat cells were withdrawn for lysis, as described above, 10^6 cells (100 μl) were taken as a function of time from the

reaction and added to 500 µl Annexin A5 binding buffer containing 10 µl Annexin A5-FluoProbes 488. After 20 min in the dark, the cells were analyzed using a Becton Dickinson FACScan equipped with CellQuest software (BD Biosciences); 10 000 events were acquired for each sample. Fluorescence emitted at the level of the undamaged cells was determined by analyzing the counts *versus* FL1-H for a gated population of intact cells, excluding debris and microparticles, delineated with the light scattering properties using forward scatter (FSC) *versus* FL1-H profiles in dot plot mode.

Platelet isolation. Freshly drawn blood was obtained from control subjects by venepuncture, using acid-citrate-dextrose formula A as an anticoagulant, and platelets were washed in 145 mM NaCl, 4 mM KCl, 0.5 mM $MgCl_2$, 0.5 mM NaH_2PO_4, 5 mM PIPES pH 6.8, and 5.5 mM glucose (washing buffer), as already described [5]. Washed platelets were resuspended in 137 mM NaCl, 2 mM KCl, 0.5 mM NaH_2PO_4, 0.5 mM $MgCl_2$, 10 mM HEPES pH 7.4, and 5.5 mM glucose (platelet reaction buffer) and used immediately.

Kinetic studies of platelet membrane remodeling using FM1–43. Platelets in reaction buffer (2 ml) containing 2 mM Ca^{2+} or Ca^{2+}-free buffer containing 0.1 mM EGTA were pre-incubated with 10 µM U0126 or vehicle for 15 min at 37°C. Membrane remodeling was then analyzed with 5 µM FM1–43 in a cuvette under stirring. Fluorescence was measured in a Spex FluoroMax fluorimeter (Spex Industries Inc., Edison, NJ), equipped with a thermostatic jacket and a stirring device. Excitation and emission wavelengths were 510 and 590 nm, respectively, and time increment between two fluorescence measurements was 1 s.

$[Ca^{2+}]_i$ measurements in platelets. Isolated platelets were incubated with 5 µM Fura-2 in washing buffer at 37°C for 45 min, washed twice and resuspended in reaction buffer. $[Ca^{2+}]_i$ changes were monitored by measuring the Fura-2 fluorescence ratio at 340/380 nm with emission at 510 nm (time increment: 2 s). Fura-2-loaded platelets were incubated in reaction buffer in the presence of 0.1 mM EGTA for experiments performed in Ca^{2+}-free buffer. Alternatively, Ca^{2+} measurements were performed with Fura-2-loaded platelets directly in the presence of 2 mM extracellular Ca^{2+}.

Activation of platelets for ERK1/2 phosphorylation analysis by Western blotting. Platelets (500 µl) were pre-incubated for 15 min with or without 10 µM U0126, and stimulated with 3 µM A23187 at 37°C. Samples (50 µl) were taken at different time intervals. The reaction was stopped by adding 5× Laemmli reducing buffer in the presence of protease inhibitors (cocktail set III, Sigma), and the samples were boiled for 2–3 min. After electrophoresis on SDS-9 % polyacrylamide gels in the Mini-PROTEAN 3 Electrophoresis Cell, the proteins were transferred onto nitrocellulose membrane for 1 h at 100 V using the Trans-Blot Electrophoretic Transfer Cell, for Western blotting.

Results

Effect of ERK inhibition on Ca^{2+} ionophore-induced PL scrambling and $[Ca^{2+}]_i$ increase in Jurkat cells. The strict time correlation between $[Ca^{2+}]_i$ increase and PL scrambling was analyzed by fluorescence imaging video microscopy, as previously described for B lymphoblasts [13]. In this method, the fluorescence of individual cells loaded with Fura-2 Ca^{2+} indicator was recorded in FM1–43-containing medium, for simultaneous assessment of $[Ca^{2+}]_i$ and membrane remodeling (see Materials and methods). FM1–43 lipophilic dye has been validated as an alternative to Annexin A5 for monitoring the rapid PL scrambling correlated with PS exposure [17, 31, 35].

In Ca^{2+}-containing reaction buffer, the addition of ionomycin produced rapid $[Ca^{2+}]_i$ increases in all Jurkat cells, as demonstrated by increases in the Fura-2 fluorescence ratios (Fig. 1A). The $[Ca^{2+}]_i$ increase preceded membrane scrambling, which occurred at different time points for each individual cell as indicated by a sharp jump in FM1–43 fluorescence. The shift in FM1–43 fluorescence corresponds to the partitioning of the dye into the anionic outer membrane leaflet, and the resulting increase in fluorescence quantum yield [36]. The FM1–43 fluorescence curves exhibited a typical shape, consisting of a peak followed by a transient decrease, as previously observed for B lymphoblasts [13]. The shape of the curves, after the initial sharp increase, indicated that molecular conformational changes occur within the membrane structure in the vicinity of the dye, leading to a transient decrease in fluorescence.

As shown by the Western blotting in Figure 1C, Ca^{2+} ionophores produced an increased in ERK phosphorylation, as compared to basal phosphorylation in this cell line. This phosphorylation was transient due to the phosphatase activation [37].

To examine the consequence of ERK pathway inactivation on the kinetics, U0126, an inhibitor of ERK phosphorylation by MEK1/2, was added to the cell medium 20 min before the ionophore. Following addition of ionomycin, the time required to reach

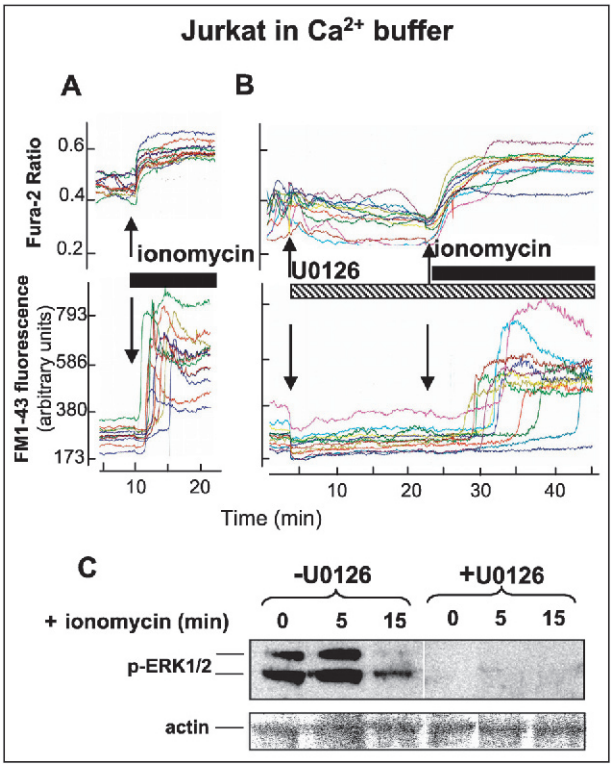

Figure 1. Effects of U0126 on intracellular Ca^{2+} concentration ($[Ca^{2+}]_i$), phospholipid (PL) scrambling and extracellular signal-regulated kinase (ERK) phosphorylation in Jurkat cells in Ca^{2+}-containing buffer. (*A*, *B*) Representative Jurkat single-cell traces simultaneously recorded for $[Ca^{2+}]_i$ increase, as shown by Fura-2 fluorescence ratios at 340/380 nm (upper traces, arbitrary units), and membrane remodeling, revealed by FM1–43 fluorescence (lower traces, arbitrary units). Traces are color coded: for an individual cell, Fura-2 fluorescence ratio (upper trace) and FM1–43 fluorescence (lower trace) are indicated by the same color. (*A*) In the absence of U0126, 2 μM ionomycin induced an increase in Fura-2 fluorescence ratio, rapidly followed by an increase in FM1–43 fluorescence. (*B*) In the continuous presence of 10 μM U0126, the onset of the increase in FM1–43 fluorescence was delayed (mean time for the onset of FM1–43 fluorescence after ionomycin addition: 2.2±1.5 min (n=26) in the absence of U0126 and 7.2±3.5 min (n=28) in the presence of U0126, $p<0.0001$). Data are representative of three independent experiments. (*C*) ERK phosphorylation analysis by Western blotting showed that ERK phosphorylation, monitored by the anti-pYpT-ERK1/2 antibody (Ab), was transiently induced in the absence of U0126 and completely inhibited in cells incubated with U0126. Identical protein loading is demonstrated by protein staining of the blot with Ponceau dye, as indicated by the actin band.

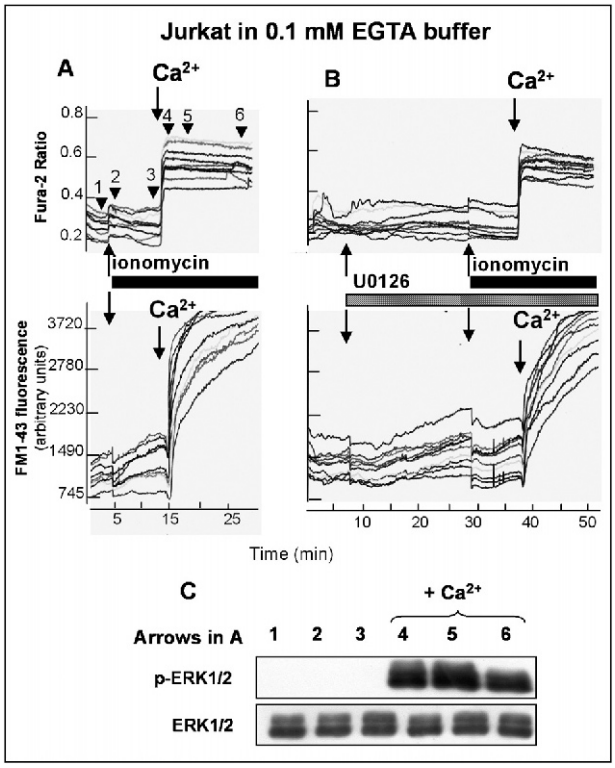

Figure 2. Effects of U0126 on $[Ca^{2+}]_i$, PL scrambling and ERK phosphorylation in Jurkat cells in Ca^{2+}-free buffer. Experimental conditions were as in Fig. 1, except that the cells were incubated in Ca^{2+}-free buffer containing 0.1 mM EGTA. Ionomycin (2 μM) was added to the buffer for 10 min before adding 1.8 mM $CaCl_2$ (arrows). (*A*) Traces in the absence of inhibitor. (*B*) U0126 (10 μM) was added 20 min prior to the addition of ionomycin followed, 10 min later, by $CaCl_2$. These data are representative of at least three independent experiments performed on different days. Results showed that for 100% cells present on the examination fields (20–30 cells) both Fura-2 fluorescence ratio and FM1–43 fluorescence increased instantly with $CaCl_2$, in the absence or presence of U0126. (*C*) Western blots illustrate the ERK phosphorylation status in Jurkat cells at different time points in the absence of inhibitor (arrowheads in *A*). Independent Western blots were performed and immunolabeled with anti-pYpT-ERK1/2, and anti-ERK1/2 Ab. Results showed that ERK phosphorylation occurred rapidly following Ca^{2+} addition.

the maximum $[Ca^{2+}]_i$ increase and the typical shifts in FM1–43 fluorescence were delayed, occurring between 5 and 20 min (Fig. 1B). As shown in Figure 1C, ERK1/2 was completely unphosphorylated in Jurkat cells incubated with U0126 (including basal phosphorylation, compare lanes 0, minus and plus U0126, in Fig. 1C). ERK1/2 remained unphosphorylated following ionophore addition, signifying that ERK activation was inhibited throughout the video microscopy experiment. Therefore, ERK inhibition delayed Ca^{2+} entry and PL scrambling, but with time both responses were overcome.

In a Ca^{2+}-free reaction buffer containing 0.1 mM EGTA, ionomycin, *per se*, did not significantly change the Fura-2 or FM1–43 fluorescence (Fig. 2). Addition of 1.8 mM $CaCl_2$ induced rapid Fura-2 and FM1–43 fluorescence increases and immediate ERK phosphorylation. Cells in which ERK phosphorylation was inhibited in the presence of U0126 exhibited similar kinetics (Fig. 2B).

Another MEK inhibitor, PD98059 (10 μM), directly induced a slow increase in FM1–43 fluorescence following addition to Jurkat cells incubated in Ca^{2+} buffer (not shown). This artifact, which was not associated with $[Ca^{2+}]_i$ increase, is another illustration

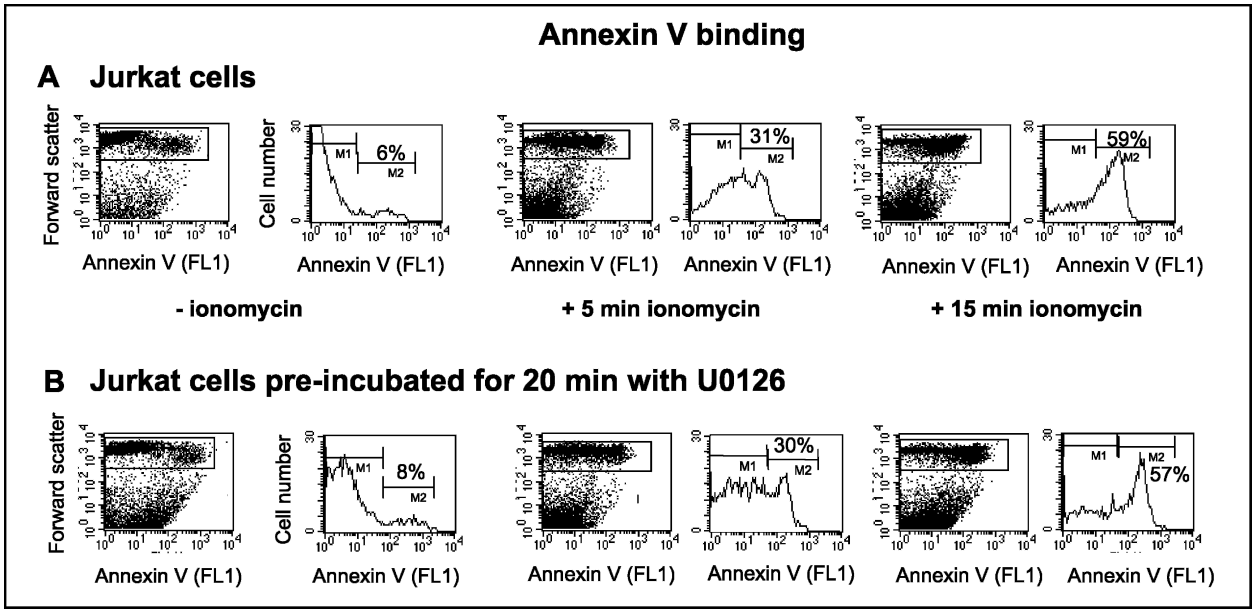

Figure 3. Flow cytometry analysis of the binding of fluorescent Annexin A5 to Jurkat cells. The cells were stimulated by 2 μM ionomycin in Ca^{2+}-containing buffer without (*A*) or with the continuous presence of 10 μM U0126 (*B*). Aliquots of 100 μl cells (10^6) withdrawn from the samples at the indicated time points were analyzed for phosphatidylserine (PS) exposure using fluorescent Annexin V-FluoProbes 488, in parallel with the determination of ERK phosphorylation shown in Figure 1C. Fluorescence histograms of the gated region on forward scatter *versus* Annexin A5 fluorescence dot plots revealed two subpopulations (M1 and M2). The percentage of the subpopulation expressing maximum Annexin A5 binding (M2) increased with time following ionomycin activation, as a result of PS exposure, and remained unchanged in the presence of U0126. The experiment is representative of three independent experiments.

that PD98059 has side effects on cell membranes independently of MEK inhibition, as reported in a different cell type [38].

Inhibition of the MAPK/ERK pathway did not prevent ionophore-induced PS exposure, demonstrated by Annexin A5 binding. To confirm the PS exposure in Jurkat cells where the MAPK/ERK pathway had been inhibited using a different method, the cells were analyzed for Annexin A5 binding by flow cytometry. ERK phosphorylation and Annexin A5 binding were assessed at the same time points following ionophore activation with or without U0126 (Fig. 3). In the absence of the inhibitor, the percentage of cells binding Annexin A5 increased rapidly (Fig. 3A), reaching 31 % positive 5 min after ionomycin addition (compared to 6 % for untreated cells), and 59 % at 15 min, but no further increase up to 30 min (not shown). In the presence of U0126, which inhibited ERK phosphorylation (Fig. 1C), the percentage of cells probed with fluorescent Annexin A5 were similar to those determined at the corresponding time points in the absence of inhibitor (Fig. 3B). Therefore, flow cytometry studies confirmed that PS exposure occurred even when ERK phosphorylation was inhibited. However, they did not reveal the heterogeneous responses, captured by video microscopy, of the individual cells in Ca^{2+} buffer (Fig. 1).

Effect of ERK inhibition on Ca^{2+} ionophore-induced PL scrambling and $[Ca^{2+}]_i$ increase in platelets. The $[Ca^{2+}]_i$ increase in Fura-2-loaded platelets in suspension and PL scrambling in the presence of FM1–43 were analyzed independently by spectrofluorimetry. Recordings of the Fura-2 ratio and FM1–43 fluorescence in Ca^{2+}-containing reaction buffer demonstrated that A23187 instantly caused both $[Ca^{2+}]_i$ increase and PL scrambling in platelets. The slope for the Fura-2 ratio curve was, however, steeper than that for FM1–43 fluorescence, indicating that $[Ca^{2+}]_i$ increase slightly preceded scrambling (Fig. 4A, B). These effects coincided with the rapid, transient ERK phosphorylation (Fig. 4C). ERK2 is the form preferentially expressed and activated in platelets [22, 23], as illustrated by the single band on the gels. ERK phosphorylation was inhibited in the presence of U0126 (Fig. 4C) and the ionophore-induced increase in $[Ca^{2+}]_i$ was attenuated (Fig. 4A). However, the PL scrambling kinetic was identical to that observed without MEK inhibition (Fig. 4B). After $[Ca^{2+}]_i$ increase, membrane scrambling occurred more rapidly in platelets than in Jurkat cells (Fig. 1A, B), whether U0126 was present or absent.

In a buffer without exogenous Ca^{2+} (containing 0.1 mM EGTA), adding ionophore to platelets instantly produced a significant transient shift in Fura-2 fluorescence (Fig. 5A). This transient peak, indicating

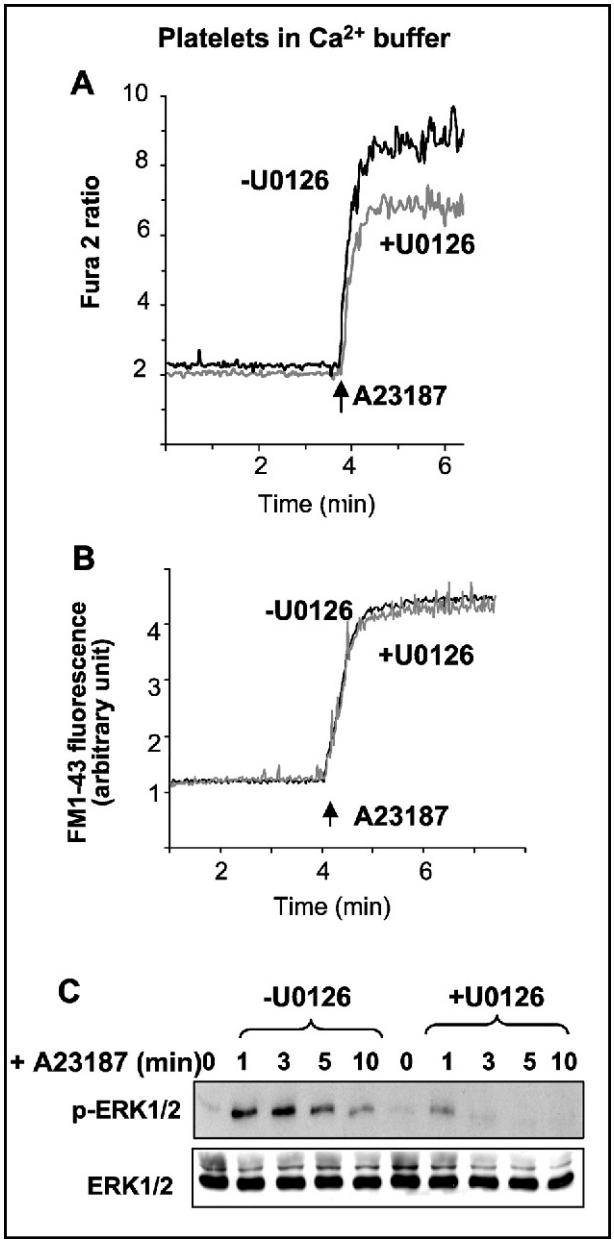

Figure 4. Effects of U0126 on $[Ca^{2+}]_i$, PL scrambling, and ERK phosphorylation in platelets incubated in Ca^{2+}-containing buffer. Platelets pre-incubated with 10 μM U0126 (gray curve), or vehicle (black curve) at 37°C for 15 min, were stimulated with Bromo-A23187 (3 μM), a non-fluorescent Ca^{2+} ionophore, in the presence of 2 mM $CaCl_2$, and analyzed in suspension by fluorimetry, as described in Materials and methods. (*A*) $[Ca^{2+}]_i$ increase, indicated by the Fura-2 fluorescence ratio. (*B*) PL scrambling monitored with FM1–43. Curves A and B are representative of four to six independent experiments. U0126 diminished cytosolic Ca^{2+} increase but did not inhibit membrane scrambling. (*C*) Aliquots were solubilized with reducing Laemmli buffer at the times indicated during the kinetics, and analyzed for ERK phosphorylation by Western blotting. Results showed that ERK2 (isoform expressed in platelets) phosphorylation probed with the anti-pY-ERK1/2 Ab was transient and inhibited in the presence of U0126. Identical protein loading was shown by labeling with anti-ERK1/2 Ab. The experiment in (*C*) is representative of three independent experiments.

mobilization of the internal Ca^{2+} pool, was associated with ERK phosphorylation (lanes 2- and 3-, Fig. 5C). Therefore, exogenous Ca^{2+} entry is not necessary for ionophore-induced ERK phosphorylation in platelets. Adding $CaCl_2$ induced Ca^{2+} entry and membrane scrambling, but no significant change in ERK phosphorylation (lanes 4- and 5-, Fig. 5C). The presence of U0126 reduced the amount of Ca^{2+} flowing into the cells (Fig. 5A) but the rapid, sharp increase in FM1–43 fluorescence, indicative of membrane scrambling, was normal (Fig. 5B). Western blotting confirmed that ERK phosphorylation was continuously inhibited in the presence of U0126 (lanes 2+ to 5+, Fig. 5C). The data revealed that inhibiting ERK phosphorylation did not prevent membrane PL scrambling in platelets, although Ca^{2+} entry was reduced.

ERK phosphorylation in B lymphoblasts. Previous experiments using the same video microscopy methods showed that Scott B lymphoblasts did not exhibit the FM1–43 fluorescence response following ionophore activation, despite a normal Ca^{2+} influx [13]. To test an initial hypothesis that a specific signal for membrane scrambling was defective in these cells, we analyzed the Ca^{2+}-ionophore-induced ERK phosphorylation pathway in normal and Scott B lymphoblasts.

As shown in Figure 6, both normal and Scott B lymphoblasts demonstrated strong basal phosphorylation of ERK1/2. This constitutive ERK activation did not depend on the cell growth medium, as similar results were obtained using cells grown in serum-free X-VIVO-15 medium and RPMI medium supplemented with 10 % FCS (medium also used for Jurkat cells, Materials and methods). Our results were thus in keeping with the fact that, after transformation, the EBV latent membrane protein 1 mediates lymphocytic cell immortalization by permanently activating Ras/MEK/ERK pathways [39].

Neither increased ERK phosphorylation nor dephosphorylation was clearly detectable in these normal and Scott B lymphoblasts following ionophore addition (Fig. 6). Overall, the data demonstrate that a high basal ERK phosphorylation is not associated with basal PS exposure, and in spite of ERK phosphorylation, Scott cells from the patient do not expose PS upon ionophore-induced Ca^{2+} entry.

Discussion

Our investigation disproved the hypothesis that activating the MAPK/ERK pathway promotes Ca^{2+}-dependent PL scrambling at the cell membrane. Firstly, our results showed that ionophore-induced

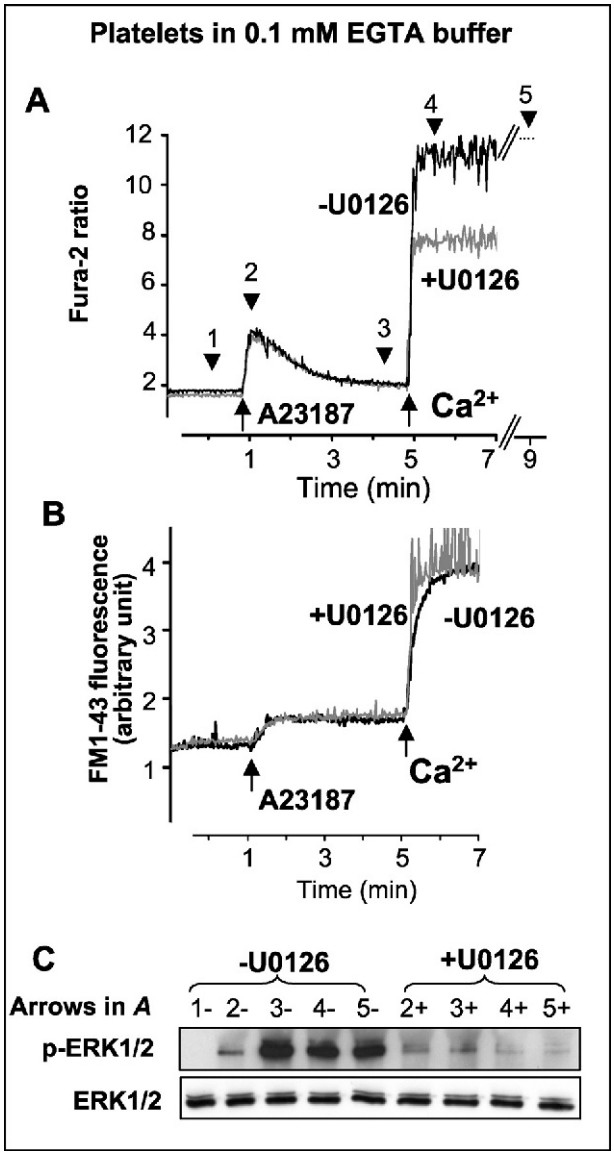

Figure 5. Effects of U0126 on $[Ca^{2+}]_i$, PL scrambling and ERK phosphorylation in platelets incubated in Ca^{2+}-free buffer. Platelets were pre-incubated with 10 μM U0126 (gray curve), or vehicle (black curve) in reaction buffer containing 0.1 mM EGTA but no exogenous Ca^{2+} at 37°C for 15 min. The sample was stimulated with 3 μM Bromo-A23187 for 4 min, then 2 mM $CaCl_2$ was added to the medium. (*A*) $[Ca^{2+}]_i$ change revealed by Fura-2 fluorescence ratio at 340/380 nm. Adding the ionophore to platelets instantly caused a significant transient shift in Fura-2 fluorescence, indicating mobilization of the internal Ca^{2+} pool. (*B*) PL scrambling detected with FM1–43. Curves A and B are representative of four to six independent experiments. U0126 decreased Ca^{2+} influx but did not inhibit membrane scrambling. (*C*) Samples (1–5) were taken at different times (arrowheads in *A*), and immediately solubilized with reducing Laemmli buffer for Western blotting. Results showed that ERK2 phosphorylation probed with anti-pY-ERK1/2 Ab did not require extracellular Ca^{2+}, and was inhibited by U0126. Identical protein loading was shown by labeling with anti-ERK1/2 Ab. The experiment in (*C*) is representative of three independent experiments.

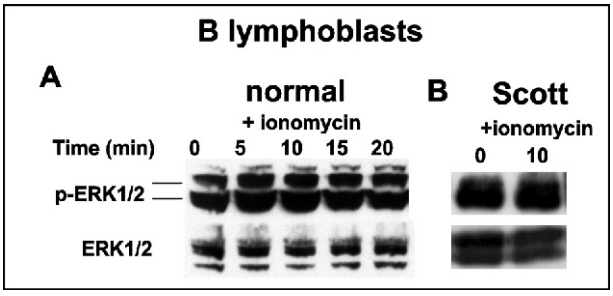

Figure 6. ERK1/2 was constitutively phosphorylated in normal and Scott B lymphoblasts. As described in Materials and methods, EBV-transformed B lymphocytes were derived from a French patient with Scott syndrome or from a healthy unrelated individual (normal). The cells (10^7 cells/ml in reaction buffer containing 1.8 mM $CaCl_2$) were activated by 2 μM ionomycin and samples taken at different times were lysed and analyzed by Western blotting with anti-pYpT-ERK1/2 Ab. Results showed that ERK was basally phosphorylated both in EBV-transformed normal and Scott cells. The membranes were stripped and re-probed with anti-ERK1/2 Ab (*A*) or a new membrane was probed (*B*). Results are representative of three experiments for each cell type.

ERK activation required Ca^{2+} influx in Jurkat cells but was independent of Ca^{2+} entry in platelets, while PS exposure required an intracellular Ca^{2+} increase in the presence of extracellular Ca^{2+}. Secondly, the A23187-induced MAPK/ERK pathway activation in platelets in Ca^{2+}-free buffer was not accompanied by PL scrambling, demonstrating that another signal, initiated by Ca^{2+} entry, was necessary for the process. Thirdly, membrane remodeling and PS exposure occurred in Jurkat cells and platelets even when ERK activation was inhibited (Figs. 1–5).

Ionomycin induces ERK1/2 activation in Jurkat cells *via* the sequential activation of a calmodulin-dependent protein kinase and $p56^{Lck}$, both proteins acting upstream from MEKs [40]. In these cells, ionophore-induced ERK phosphorylation correlated with Ca^{2+} entry, as shown in experiments performed in the presence of exogenous Ca^{2+}, or following the addition of $CaCl_2$ to EGTA-containing medium (Figs. 1C, 2C). In contrast, ERK phosphorylation in platelets was induced by ionophores, together with Ca^{2+}-store depletion and no external Ca^{2+} was required (Fig. 5C). In line with this result, other studies showed that ERK phosphorylation was induced in platelets, loaded with the intracellular Ca^{2+} chelator BAPTA/AM in a Ca^{2+}-free medium, by thapsigargin, which depletes Ca^{2+} stores from the endoplasmic reticulum [27]. Therefore, our data confirm that Ca^{2+} ionophores activate ERK *via* different signals in lymphoblastic cells and platelets, whereas PL scrambling presumably relies on a common pathway in both cell types (as schematized in Fig. 7).

We observed that in Jurkat cells the lag between $[Ca^{2+}]_i$ increase and FM1–43 fluorescence changes

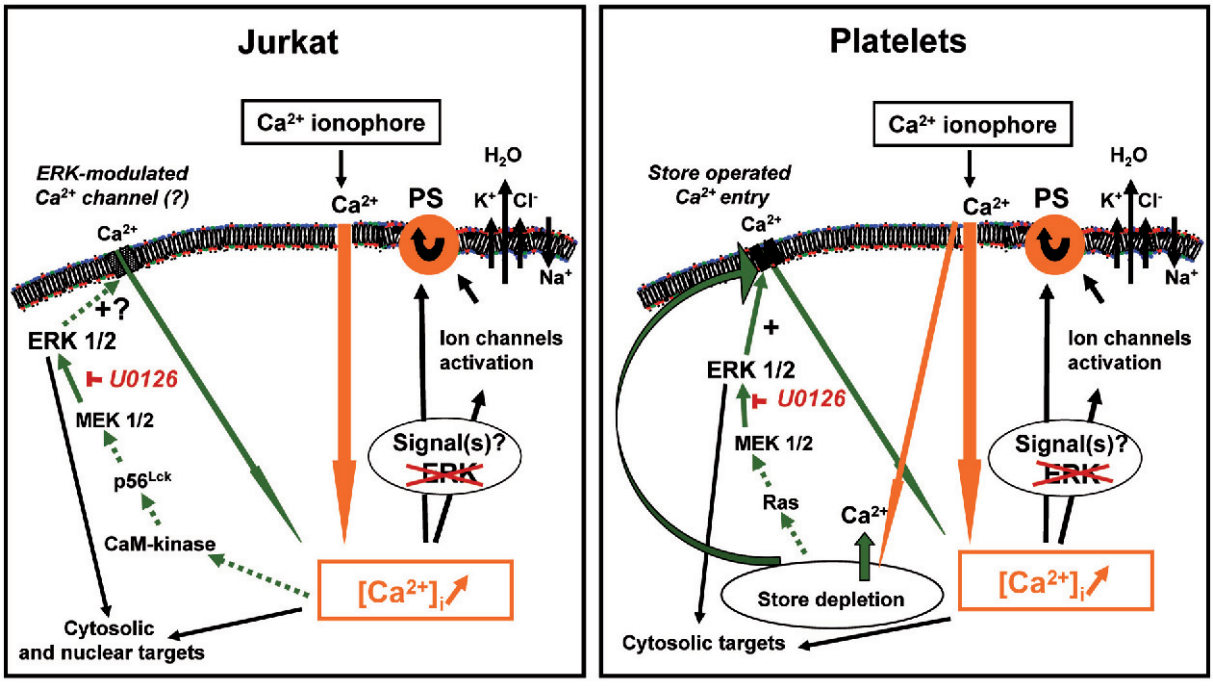

Figure 7. Schematic representation of ERK activation and PS exposure induced by Ca^{2+} ionophores in Jurkat cells and in platelets. ERK activation occurs through different pathways in platelets and lymphocytes, requesting Ca^{2+} entry in lymphocytes, and being induced without a need for external Ca^{2+} in platelets. In T cells, Ca^{2+} ionophore-induced ERK phosphorylation occurs *via* $p56^{Lck}$ and calmodulin (CaM)-kinase [40]. Our data suggest that the MAPK/ERK pathway modulates cytosolic Ca^{2+} increase in Jurkat cells, supposedly by regulating a putative channel involved in Ca^{2+} entry. In platelets in Ca^{2+}-free buffer, Ca^{2+} ionophore discharges Ca^{2+} from internal pools including ER stores (store depletion), as shown in Fig. 5A. In platelets, the store depletion signal is associated with the activation, independently of external Ca^{2+}, of Ras and the MAPK/ERK pathway, which in turns modulates store-operated calcium channels [27]. Both in Jurkat cells and platelets, membrane scrambling and PS exposure occur even when ERK activation is inhibited and are dependent on the level of $[Ca^{2+}]_i$ increase. Also shown is Ca^{2+}-induced stimulation of ion channels, resulting in K^+ and Cl^- loss, Na^+ entry, cell dehydration, change in lipid packing, all concomitant with PL scrambling [16]. ERK activation and $[Ca^{2+}]_i$ increase stimulate multiple other pathways that are not schematized here.

observed in Ca^{2+}-containing buffer (Fig. 1A) did not occur when ionomycin and Ca^{2+} were added to the cells incubated in EGTA-containing buffer (Fig. 2A). Similar results were observed in the presence of U0126 (compare Fig. 2A and B). Therefore, the efflux or influx of various ions due to the pumping of Ca^{2+} out of the cells by external EGTA in the medium facilitates the activation of the scrambling mechanism, since cells lose K^+ and gain Na^+ in Ca^{2+}-free medium [41]. Because K^+ efflux and Na^+ influx were proposed to be involved in the PS exposure process [16, 42], it may be that the novel ionic environment had already primed the activation of the PL scrambling. Therefore, scrambling and FM1–43 fluorescence increase occurred instantaneously with Ca^{2+} entry.

Interestingly, incubation with U0126, which effectively inhibited ERK phosphorylation throughout the experiments, delayed membrane remodeling when Jurkat cells were analyzed in Ca^{2+}-containing buffer, by delaying $[Ca^{2+}]_i$ increase (Fig. 1B). The Ca^{2+} signal induced by Ca^{2+} ionophores has been shown to consist of several components, including the activation of influx *via* native Ca^{2+} channels, a phospholipase C-dependent mobilization of Ca^{2+} from intracellular stores, and a store-regulated mechanism [43]. Our data suggest that U0126 inhibits one or more components involved in the $[Ca^{2+}]_i$ increase induced by the ionophore concentrations of micromolar range necessary to stimulate membrane scrambling in lymphocytic cells [9, 17]. The mechanism involved could be the inhibition of a Ca^{2+} channel. Activated ERK regulates Ca^{2+} channels by phosphorylation, as demonstrated in neurons [44]. However, with time, the effect of U0126 retarding $[Ca^{2+}]_i$ increase in Jurkat cells was overcome, and membrane scrambling was not blocked.

The p-ERK1/2 status in the specific B lymphocytes immortalized in our laboratory [10] correlates with the fact that EBV latent membrane protein 1 mediates cell transformation by permanently activating Ras/MEK/ERK pathways [39]. Data showed that the mutation in the Scott B lymphoblasts from a French patient does not alter ERK phosphorylation upon EBV-induced activation of Ras/MEK/ERK pathways.

The strong basal phosphorylation of ERK1/2 in the B lymphoblasts is not associated with basal PS exposure, and, in spite of ERK activation, the Scott cells do not expose PS upon ionophore-induced Ca^{2+} entry.

As the MAPK/ERK pathway is up-regulated in a variety of solid tumors, multikinase inhibitors, shown to inhibit ERK phosphorylation *in vivo*, have been successfully developed as anticancer drugs. These drugs are particularly effective in treating renal cell carcinomas and a type of acute myelogenous leukemia [45–47]. Clinical studies demonstrated diminished platelet counts in some patients. Our results suggest that the therapeutic use of ERK activation inhibitors in cancer patients is unlikely to cause an exacerbated tendency to bleeding.

New pathways should now be explored to discover how Ca^{2+} entry controls PS translocation. Importantly, the rapid surface exposure of PS following stimulation with Ca^{2+} ionophores or *via* cell-specific Ca^{2+} influx-inducing receptors is associated with cell shrinkage, also a hallmark of apoptosis. Shrinkage results from cell dehydration involving a Ca^{2+}-activated efflux of K^+ and Cl^- ions [16, 48, 49]. In platelets, PS exposure induced *in vitro* by collagen plus thrombin also involves K^+ (Gardos) channels [50]. Other studies showed that Na^+ influx *via* a Na^+/H^+ exchanger is involved in PL scrambling in platelets stimulated by the physiological agonists thrombin or collagen [42].

Although existing models assume that the translocation of lipids in an asymmetrical membrane is due to transmembrane ion transport [16] or depends on local effects, such as the induced formation of transient pores, the role of proteins catalyzing PS translocation is still an extensively debated subject (reviewed in [14]). The defect in Scott syndrome suggests the existence of a strategic founding element for the remodeling process, which may be a membrane ion channel or a $[Ca^{2+}]_i$ increase-dependent signaling underlying ion movements, independently of MAPK/ERK activation.

Acknowledgments. A. Arachiche is supported by a grant from the Nouvelle Société Française d'Athérosclérose. This work was funded by a grant from the Fondation de France No. 2005 005347, and financed by INSERM, Université Paris-Sud (Le Kremlin-Bicêtre), and Université Victor Segalen (Bordeaux). We are particularly grateful to Dr. Laurent Combettes (INSERM UMR-S757, Université Paris-Sud, Orsay), for his essential help in setting up the video microscopy studies. We acknowledge Dr. Marijke Bryckaert for having shared with us her expertise in interpreting the Western blots for ERK phosphorylation in platelets. We thank Dr. Jean-Marie Freyssinet and Dr. Thierry Letellier for their support, Dr. Dominique Chesnoy-Marchais and Olivier Trassard for helpful discussions. We are extremely grateful to the Fondation de France and the Nouvelle Société Française d'Athérosclérose for their essential financial support.

1 Bevers, E. M., Comfurius, P. and Zwaal, R. F. (1983) Changes in membrane phospholipid distribution during platelet activation. Biochim. Biophys. Acta 736, 57–66.
2 Schlegel, R. A. and Williamson, P. (2001) Phosphatidylserine, a death knell. Cell Death Differ. 8, 551–563.
3 Adayev, T., Estephan, R., Meserole, S., Mazza, B., Yurkow, E. J. and Banerjee, P. (1998) Externalization of phosphatidylserine may not be an early signal of apoptosis in neuronal cells, but only the phosphatidylserine-displaying apoptotic cells are phagocytosed by microglia. J. Neurochem. 71, 1854–1864.
4 Comfurius, P., Senden, J. M., Tilly, R. H., Schroit, A. J., Bevers, E. M. and Zwaal, R. F. (1990) Loss of membrane phospholipid asymmetry in platelets and red cells may be associated with calcium-induced shedding of plasma membrane and inhibition of aminophospholipid translocase. Biochim. Biophys. Acta 1026, 153–160.
5 Dachary-Prigent, J., Freyssinet, J. M., Pasquet, J. M., Carron, J. C. and Nurden, A. T. (1993) Annexin V as a probe of aminophospholipid exposure and platelet membrane vesiculation: A flow cytometry study showing a role for free sulfhydryl groups. Blood 81, 2554–2565.
6 Weiss, H. J., Vicic, W. J., Lages, B. A. and Rogers, J. (1979) Isolated deficiency of platelet procoagulant activity. Am. J. Med. 67, 206–213.
7 Sims, P. J., Wiedmer, T., Esmon, C. T., Weiss, H. J. and Shattil, S. J. (1989) Assembly of the platelet prothrombinase complex is linked to vesiculation of the platelet plasma membrane. Studies in Scott syndrome: An isolated defect in platelet procoagulant activity. J. Biol. Chem. 264, 17049–17057.
8 Bevers, E. M., Wiedmer, T., Comfurius, P., Shattil, S. J., Weiss, H. J., Zwaal, R. F. and Sims, P. J. (1992) Defective Ca^{2+}-induced microvesiculation and deficient expression of procoagulant activity in erythrocytes from a patient with a bleeding disorder: A study of the red blood cells of Scott syndrome. Blood 79, 380–388.
9 Kojima, H., Newton-Nash, D., Weiss, H. J., Zhao, J., Sims, P. J. and Wiedmer, T. (1994) Production and characterization of transformed B-lymphocytes expressing the membrane defect of Scott syndrome. J. Clin. Invest. 94, 2237–2244.
10 Toti, F., Satta, N., Fressinaud, E., Meyer, D. and Freyssinet, J. M. (1996) Scott syndrome, characterized by impaired transmembrane migration of procoagulant phosphatidylserine and hemorrhagic complications, is an inherited disorder. Blood 87, 1409–1415.
11 Munnix, I. C., Harmsma, M., Giddings, J. C., Collins, P. W., Feijge, M. A., Comfurius, P., Heemskerk, J. W. and Bevers, E. M. (2003) Store-mediated calcium entry in the regulation of phosphatidylserine exposure in blood cells from Scott patients. Thromb. Haemost. 89, 687–695.
12 Elliott, J. I., Mumford, A. D., Albrecht, C., Collins, P. W., Giddings, J. C., Higgins, C. F., Tuddenham, E. G. and McVey, J. H. (2004) Characterisation of lymphocyte responses to Ca^{2+} in Scott syndrome. Thromb. Haemost. 91, 412–415.
13 Galitzine, M., Capiod, T., Le Deist, F., Meyer, D., Freyssinet, J. M. and Kerbiriou-Nabias, D. (2005) Ca^{2+} ionophores trigger membrane remodeling without a need for store-operated Ca^{2+} entry. Biochem. Biophys. Res. Commun. 327, 335–341.
14 Devaux, P. F., Lopez-Montero, I. and Bryde, S. (2006) Proteins involved in lipid translocation in eukaryotic cells. Chem. Phys. Lipids 141, 119–132.
15 Wolfs, J. L., Comfurius, P., Rasmussen, J. T., Keuren, J. F., Lindhout, T., Zwaal, R. F. and Bevers, E. M. (2005) Activated scramblase and inhibited aminophospholipid translocase cause phosphatidylserine exposure in a distinct platelet fraction. Cell. Mol. Life Sci. 62, 1514–1525.
16 Elliott, J. I., Sardini, A., Cooper, J. C., Alexander, D. R., Davanture, S., Chimini, G. and Higgins, C. F. (2006) Phosphatidylserine exposure in B lymphocytes: A role for lipid packing. Blood 108, 1611–1617.
17 Wurth, G. A. and Zweifach, A. (2002). Evidence that cytosolic calcium increases are not sufficient to stimulate phospholipid scrambling in human T-lymphocytes. Biochem. J. 362, 701–708.

18 Keuren, J. F., Wielders, S. J., Ulrichts, H., Hackeng, T., Heemskerk, J. W., Deckmyn, H., Bevers, E. M. and Lindhout, T. (2005) Synergistic effect of thrombin on collagen-induced platelet procoagulant activity is mediated through protease-activated receptor-1. Arterioscler. Thromb. Vasc. Biol. 25, 1499–1505.

19 Kunzelmann-Marche, C., Freyssinet, J. M. and Martinez, M. C. (2002) Loss of plasma membrane phospholipid asymmetry requires raft integrity. Role of transient receptor potential channels and ERK pathway. J. Biol. Chem. 277, 19876–19881.

20 Murphy, L. O. and Blenis, J. (2006) MAPK signal specificity: The right place at the right time. Trends Biochem. Sci. 31, 268–275.

21 Li, Z., Xi, X. and Du, X. (2001) A mitogen-activated protein kinase-dependent signaling pathway in the activation of platelet integrin αIIbβ3. J. Biol. Chem. 276, 42226–42232.

22 Pawlowski, M., Ragab, A., Rosa, J. P. and Bryckaert, M. (2002) Selective dephosphorylation of the threonine(183) residue of ERK2 upon αIIbβ3 engagement in platelets. FEBS Lett. 521, 145–151.

23 Oury, C., Toth-Zsamboki, E., Vermylen, J. and Hoylaerts, M. F. (2002) P2X1-mediated activation of extracellular signal-regulated kinase 2 contributes to platelet secretion and aggregation induced by collagen. Blood 100, 2499–2505.

24 Oury, C., Daenens, K., Hu, H., Toth-Zsamboki, E., Bryckaert, M. and Hoylaerts, M. F. (2006) ERK2 activation in arteriolar and venular murine thrombosis: Platelet receptor GPIb vs. P2X1. J. Thromb. Haemost. 4, 443–452.

25 Papkoff, J., Chen, R. H., Blenis, J. and Forsman, J. (1994) p42 mitogen-activated protein kinase and p90 ribosomal S6 kinase are selectively phosphorylated and activated during thrombin-induced platelet activation and aggregation. Mol. Cell. Biol. 14, 463–472.

26 Borsch-Haubold, A. G., Kramer, R. M. and Watson, S. P. (1996) Inhibition of mitogen-activated protein kinase kinase does not impair primary activation of human platelets. Biochem. J. 318, 207–212.

27 Rosado, J. A. and Sage, S. O. (2001) Role of the ERK pathway in the activation of store-mediated calcium entry in human platelets. J. Biol. Chem. 276, 15659–15665.

28 Nadal-Wollbold, F., Pawlowski, M., Levy-Toledano, S., Berrou, E., Rosa, J. P. and Bryckaert, M. (2002) Platelet ERK2 activation by thrombin is dependent on calcium and conventional protein kinases C but not Raf-1 or B-Raf. FEBS Lett. 531, 475–482.

29 McNicol, A. and Jackson, E. C. (2003) Inhibition of the MEK/ERK pathway has no effect on agonist-induced aggregation of human platelets. Biochem. Pharmacol. 65, 1243–1250.

30 Yacoub, D., Theoret, J. F., Villeneuve, L., Abou-Saleh, H., Mourad, W., Allen, B. G. and Merhi, Y. (2006) Essential role of protein kinase C delta in platelet signaling, αIIbβ3 activation, and thromboxane A2 release. J. Biol. Chem. 281, 30024–30035.

31 Williamson, P., Christie, A., Kohlin, T., Schlegel, R. A., Comfurius, P., Harmsma, M., Zwaal, R. F. and Bevers, E. M. (2001) Phospholipid scramblase activation pathways in lymphocytes. Biochemistry 40, 8065–8072.

32 Balasubramanian, K., Mirnikjoo, B. and Schroit, A. J. (2007) Regulated externalization of phosphatidylserine at the cell surface: Implications for apoptosis. J. Biol. Chem. 282, 18357–18364.

33 Erdahl, W. L., Chapman, C. J., Taylor, R. W. and Pfeiffer, D. R. (1994) Ca^{2+} transport properties of ionophores A23187, ionomycin, and 4-BrA23187 in a well defined model system. Biophys. J. 66, 1678–1693.

34 Schote, U. and Seelig, J. (1998) Interaction of the neuronal marker dye FM1–43 with lipid membranes. Thermodynamics and lipid ordering. Biochim. Biophys. Acta 1415, 135–146.

35 Zweifach, A. (2000) FM1–43 reports plasma membrane phospholipid scrambling in T-lymphocytes. Biochem. J. 349, 255–260.

36 Cousin, M. A. (2008) Use of FM1–43 and other derivatives to investigate neuronal function. In: *Current Protocols in Neuroscience*, Chapter 2, Unit 2 6, Wiley Interscience, New York.

37 Pouyssegur, J., Volmat, V. and Lenormand, P. (2002) Fidelity and spatio-temporal control in MAP kinase (ERKs) signalling. Biochem. Pharmacol. 64, 755–763.

38 Gould, M. C. and Stephano, J. L. (2000) Inactivation of Ca^{2+} action potential channels by the MEK inhibitor PD98059. Exp. Cell Res. 260, 175–179.

39 Roberts, M. L. and Cooper, N. R. (1998) Activation of a ras-MAPK-dependent pathway by Epstein-Barr virus latent membrane protein 1 is essential for cellular transformation. Virology 240, 93–99.

40 Franklin, R. A., Atherfold, P. A. and McCubrey, J. A. (2000) Calcium-induced ERK activation in human T lymphocytes occurs *via* p56Lck and CaM-kinase. Mol. Immunol. 37, 675–683.

41 Morrill, G. A. and Robbins, E. (1967) The role of calcium in the regulation of the steady-state levels of sodium and potassium in the HeLa cell. J. Gen. Physiol. 50, 781–792.

42 Bucki, R., Pastore, J. J., Giraud, F., Janmey, P. A. and Sulpice, J. C. (2006) Involvement of the Na^+/H^+ exchanger in membrane phosphatidylserine exposure during human platelet activation. Biochim. Biophys. Acta 1761, 195–204.

43 Dedkova, E. N., Sigova, A. A. and Zinchenko, V. P. (2000) Mechanism of action of calcium ionophores on intact cells: Ionophore-resistant cells. Membr. Cell Biol. 13, 357–368.

44 Martin, S. W., Butcher, A. J., Berrow, N. S., Richards, M. W., Paddon, R. E., Turner, D. J., Dolphin, A. C., Sihra, T. S. and Fitzgerald, E. M. (2006). Phosphorylation sites on calcium channel α1 and β subunits regulate ERK-dependent modulation of neuronal N-type calcium channels. Cell Calcium. 39, 275–292.

45 Kohno, M. and Pouyssegur, J. (2006) Targeting the ERK signaling pathway in cancer therapy. Ann. Med. 38, 200–211.

46 Escudier, B., Eisen, T., Stadler, W. M., Szczylik, C., Oudard, S., Siebels, M., Negrier, S., Chevreau, C., Solska, E., Desai, A. A., Rolland, F., Demkow, T., Hutson, T. E., Gore, M., Freeman, S., Schwartz, B., Shan, M., Simantov, R. and Bukowski, R. M. (2007) Sorafenib in advanced clear-cell renal-cell carcinoma. N. Engl. J. Med. 356, 125–134.

47 Zhang, W., Konopleva, M., Shi, Y. X., McQueen, T., Harris, D., Ling, X., Estrov, Z., Quintas-Cardama, A., Small, D., Cortes, J. and Andreeff, M. (2008) Mutant FLT3: A direct target of sorafenib in acute myelogenous leukemia. J. Natl. Cancer Inst. 100, 184–198.

48 Elliott, J. I. and Higgins, C. F. (2003) IKCa1 activity is required for cell shrinkage, phosphatidylserine translocation and death in T lymphocyte apoptosis. EMBO Rep. 4, 189–194.

49 Taylor, S. R., Gonzalez-Begne, M., Dewhurst, S., Chimini, G., Higgins, C. F., Melvin, J. E. and Elliott, J. I. (2008) Sequential shrinkage and swelling underlie P2X7-stimulated lymphocyte phosphatidylserine exposure and death. J. Immunol. 180, 300–308.

50 Wolfs, J. L., Wielders, S. J., Comfurius, P., Lindhout, T., Giddings, J. C., Zwaal, R. F. and Bevers, E. M. (2006) Reversible inhibition of the platelet procoagulant response through manipulation of the Gardos channel. Blood 108, 2223–2228.